

Supplementary Information

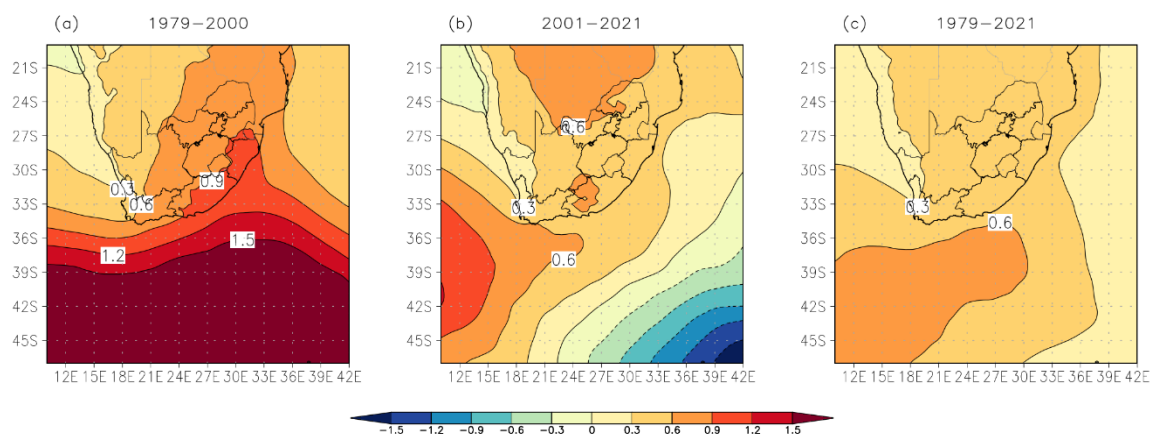
Extreme event attribution using km-scale simulations reveals the pronounced role of climate change in the Durban floods

Francois A. Engelbrecht¹, Jessica Steinkopf¹, Nicolette Chang^{1,2}, Sophie Biskop³, Johan Malherbe^{1,4}, Christien J. Engelbrecht^{5,6}, Stefan Grab⁷, Alize le Roux⁸, Coleen Vogel¹, Jonathan Padavatan¹, Marcus Thatcher⁹ and John L. McGregor^{1,9}

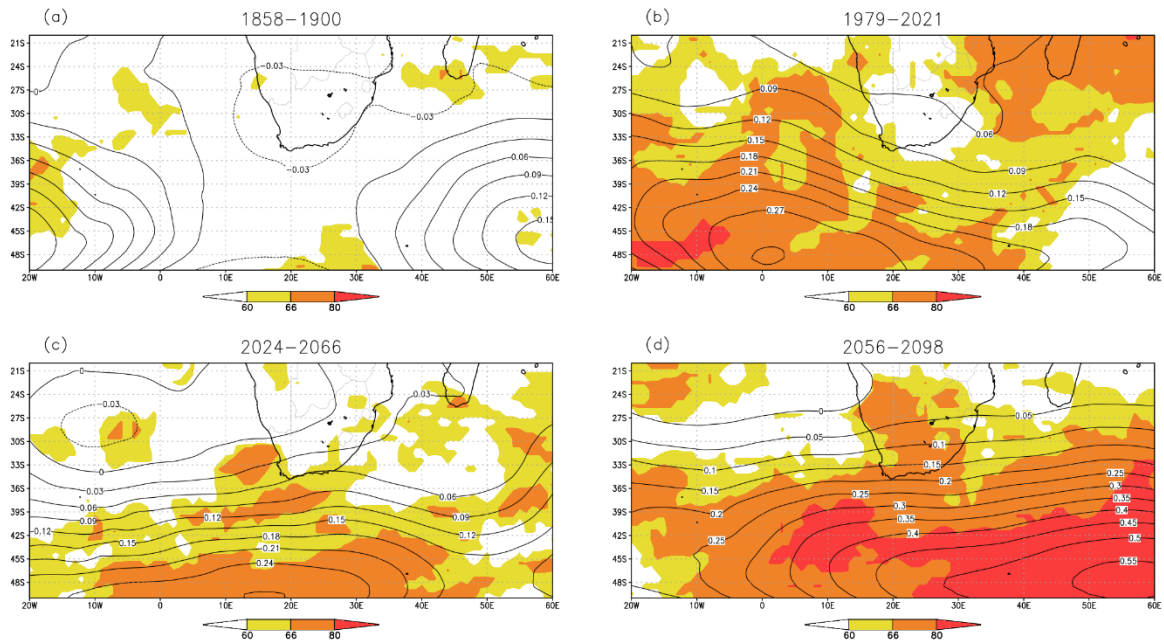
1. Global Change Institute, University of the Witwatersrand, Johannesburg, South Africa
2. Council for Scientific and Industrial Research, Southern Ocean Carbon-Climate Observatory, Cape Town, South Africa
3. Department of Geography, Friedrich Schiller University Jena, Jena, Germany
4. Agricultural Research Council, Pretoria, South Africa
5. South African Weather Service, Pretoria, South Africa
6. Department of Geography, Geoinformatics and Meteorology, University of Pretoria, Pretoria, South Africa
7. School of Geography, Archaeology & Environmental Studies, University of the Witwatersrand, Johannesburg, South Africa
8. Institute for Security Studies, Pretoria, South Africa
9. Commonwealth Scientific and Industrial Research Organisation, Melbourne, Australia

This file includes:

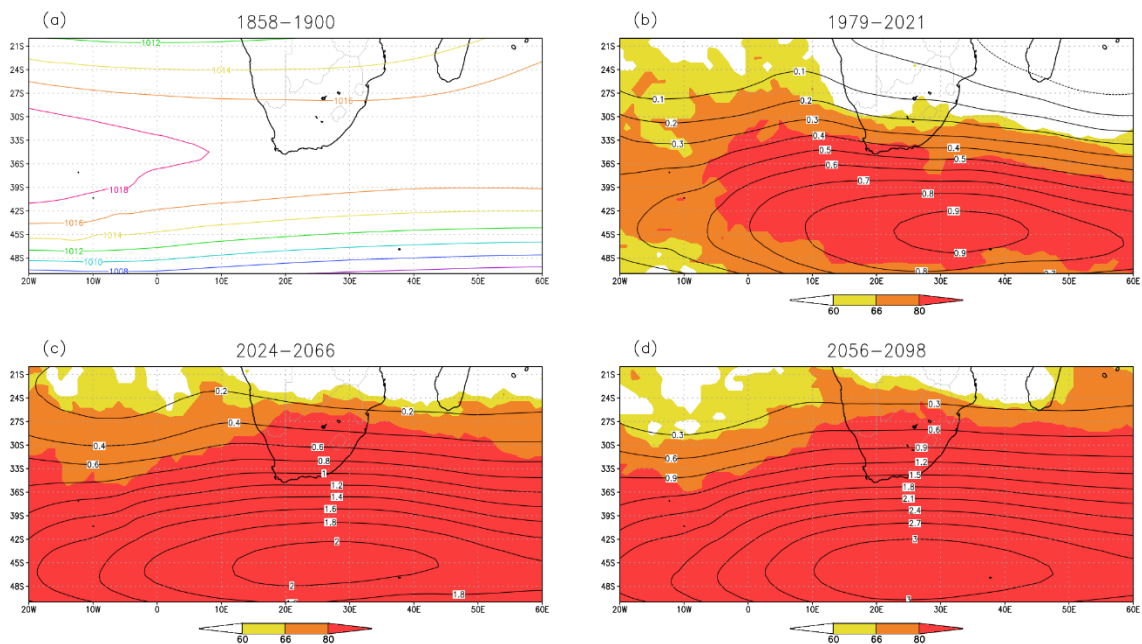
Supplementary Figures 1 to 3, and the list of CMIP6 models used to construct Supplementary Figures 2 and 3 (Supplementary Note 1).



Supplementary Figure 1: Trends in sea-level pressure (hPa/decade) for the month of April over southern Africa and surrounding oceans, as derived from ERA5-reanalysis data, for (a) 1979-2000, (b) 2000-2021 and (c) 1979-2021.



Supplementary Figure 2: Ensemble average of trends in sea-level pressure (hPa/decade, contours) as simulated by 36 CMIP6 GCMs, for the periods of (a) 1858-1900, (b) 1979-2021, (c) 2024-2066 and (d) 2056-2098 under SSP3-7.0. The shading shows model agreement in terms of the direction of change of the ensemble average.



Supplementary Figure 3: (a) Ensemble average of April sea-level pressure simulated by 36 CMIP6 for 1858-1900, and the ensemble average of changes in sea-level pressure (hPa, contours) projected by the same models under SSP3-7.0, for the periods (b) 1979-2021, (c) 2024-2066 and (d) 2056-2098 relative to 1858-1900. The shading shows model agreement in terms of the direction of change of the ensemble average.

Supplementary Note 1: List of CMIP6 models used to construct Supplementary Figures 1 and 3

The size of the ensemble used was determined by data availability on the German DKRZ data server Levante, one of the Earth System Grid Federation data servers. The models included needed to have available simulations for the historical period and projection under SSP3-7.0. Simulations from the following 36 models were analysed:

ACCESS-CM2, ACCESS-ESM1-5, AWI-CM-1-1-MR, BCC-CSM2-MR, CAMS-CSM1-0, CanESM5-CanOE, CanESM5, CAS-ESM2-0, CESM2-WACCM, CMCC-CM2-SR5, CMCC-ESM2, CNRM-CM6-1-HR, CNRM-CM6-1, CNRM-ESM2-1, EC-Earth3-AerChem, EC-Earth3, EC-Earth3-Veg-LR, EC-Earth3-Veg, FGOALS-f3-L, FGOALS-g3, GFDL-ESM4, IITM-ESM, INM-CM4-8, INM-CM5-0, IPSL-CM5A2-INCA, IPSL-CM6A-LR, KACE-1-0-G, MIROC6, MIROC-ES2L, MPI-ESM1-2-HR, MPI-ESM1-2-LR, MRI-ESM2-0, NorESM2-LM, NorESM2-MM, TaiESM1, UKESM1-0-LL.